

# BRDF Prediction Using Surface Micro-Roughness Measurements

Juan Irizar, Dr. Bernd Harnisch

**Abstract**—Straylight assessment and minimization are standard tasks in the design of high performance optical instruments. An important variable in this regard is the scattering profile of the instrument's optical surfaces. In the case of reflective samples, this is commonly specified through the Bidirectional Reflectance Distribution Function (BRDF). In spite of their widespread use, BRDF experimental measurements are challenging and time consuming. Thus, alternatives that allow for accurate approximations of the BRDF are attractive. This work explores the Rayleigh-Rice vector perturbation theory (RR) as a means to accurately and efficiently determine the BRDF of an optical reflective sample. Specifically, aerial topography interferometric measurements are used to compute the BRDF. The predicted scattering profiles are consequently compared to experimental BRDF measurements. Based on these results, it is concluded that the RR method is a promising technique to specify the scattering characteristics of an optical sample within  $\pm 0.65$  orders of magnitude

**Index Terms**—BRDF, Surface Quality, scattering, surface roughness, optical surface quality

## I. INTRODUCTION

OPTICAL scattering from optical reflective surfaces is of paramount importance in the design of high performance optical instruments. In general, scattering from these samples arises mainly from the surface topography and is best specified through the Bidirectional Reflectance Distribution Function (BRDF). The BRDF is experimentally determined by illuminating the sample with a collimated beam at an angle  $\theta_i$  as shown in Figure 1. A detector is then scanned through a variety of inclination angles  $\theta_s$ , along a plane defined by the azimuthal angle  $\phi$ . For every inclination angle  $\theta_s$ , the BRDF is defined as [1]:

$$BRDF(\theta_s, \phi) \equiv \frac{P_s / \Omega_s}{P_i \cos \theta_s} \quad (1)$$

Where  $P_s$  is the scattered power reaching the detector,  $\Omega_s$  is the solid angle of collection, and  $P_i$  is the incident power on the surface. Experimental BRDF measurements have two major drawbacks: First, they are time consuming with experimental times in the range of several hours not being uncommon. Second, a variety of experimental factors (convolution effects between the scattered signal and the detector aperture, calibration inaccuracies, instrument signature contamination, detector non-linearity, and mechanical errors) require a detailed knowledge of instrumentation which might be lacking in non-specialized optical laboratories.

Juan Irizar is with the Department of Optical Design and Performance at ASTRIUM (EADS), Munich, Germany

Bernd Harnisch is with the Department of Mechatronics and Optics at the European Space Agency (ESA), Noordwijk, Netherlands, e-mail: bernd.harnisch@esa.int.

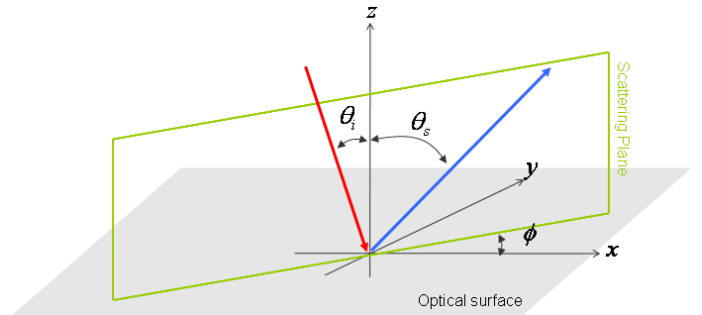


Figure 1. BRDF geometry

For a variety of applications, these two drawbacks may be overcome by approximating the BRDF using theoretical models that relate surface topography parameters to scattering profiles. For example, one of the most widely utilized approaches is the ABC or K-correlation model. It specifies the BRDF of an isotropic sample as a function of its Root Mean Square (RMS) roughness and the typical surface wavelength. Another commonly used alternative is the Harvey-Shack model [2], [1].

The present work sets out to investigate the accuracy of the Rayleigh-Rice vector perturbation theory (RR model) in predicting the BRDFs of a variety of experimental samples. The three main advantages of the RR model over other approaches (ABg or Harvey-Shack) are: a) The possibility of studying isotropic as well as anisotropic samples; b) The ability to generate scattering profiles across 3D space; c) Polarization effects in the scattered light may be taken into account.

While the RR model was developed in the late 1970s, simpler scattering models such as the ABg model, have been favored in predicting scattering profiles. The main reason behind this may be the lack of computational power in previous decades. However, using current commercial engineering software packages, the computations involved in the RR model may be easily implemented.

## II. THEORY

Let  $z(x, y)$  be a surface topography map of an optical sample within an area of  $L \cdot L$  ( $m^2$ ). The sample's Power Spectral Density function is then defined as [1]:

$$S(f_x, f_y) = \lim_{L \rightarrow \infty} \left| \int_{L/2}^{L/2} \int_{L/2}^{L/2} z(x, y) \cdot \exp(-j \cdot 2\pi [f_x x + f_y y]) dx dy \right|^2 \quad (2)$$

The PSD is the two dimensional frequency space representation of the surface topography and it is directly linked to the

optical scattering distribution from the sample. Specifically, the RR model states that the BRDF at a specific point in 3D space, specified by the coordinates  $(\theta_s, \phi_s)$ , is given by the following relation:

$$BRDF(\theta_s, \phi_s) = \frac{16\pi^2}{\lambda^4} \cdot \cos(\theta_i) \cdot \cos^2(\theta_s) \cdot Q \cdot S(f_x, f_y) \quad (3)$$

where  $\lambda$  is the incident radiation wavelength (m),  $Q$  is the reflectivity polarization factor (dimensionless). The frequencies  $f_x$  and  $f_y$  are related to other optical and geometrical parameters through the following equations:

$$f_x = \frac{\sin\theta_s \cos\phi_s}{\lambda} - \frac{\sin\theta_i}{\lambda} \quad (4)$$

$$f_y = \frac{\sin\theta_s \cos\phi_s}{\lambda} \quad (5)$$

It is important to note that Eq. 3 is derived under three key assumptions regarding the sample under investigation [1]. The sample must be: clean, a front-surface reflector, and smooth. Cleanliness restriction implies that there is a negligible contribution from contaminants on the surface to the scattering profile. A sample is a front-surface reflector if the scattering is mostly generated by surface topography with minimal contributions from sub-surface bulk or defects. Finally, the smoothness criterion implies that surface height variations are small when compared to the wavelength of the illumination.

The calculations described by the above equations may be implemented in a standard matrix-based engineering package such as MatLAB by appropriately discretizing them.

### III. MEASUREMENTS

At the time of the present study, 15 different samples developed with a variety of manufacturing techniques and differing polishing quality were available. First, BRDF experimental measurements were carried out on each sample. By using different combinations of input wavelength and angle of incidence, 50 different BRDF curves were obtained. The BRDF measurements were performed with a Complete Angle Scatter Instrument (CASI) manufactured by Schmitt Measurement Systems of Portland, Oregon, USA. Key instrument specifications are summarized in Table I.

Table I  
BRDF INSTRUMENT SPECIFICATION

Parameter	Value
Laser wavelengths (nm)	325,632.8,1064,3390
Power available (mW)	50,2,250,4.9
Spot size in FWHM (mm)	2.0
Angles of incidence (deg)	3,30,60
Angular resolution (deg)	0.001
System Accuracy	5 %
Repeatability	2%
Sample x-y motion (arcsec)	$\pm 3$
Detector apertures (microns)	278 or 1027

Consequently, the sample surface topography was experimentally measured using contactless White Light Interferometry (WLI) at a variety of magnifications. These measurements

were carried out in a Zygo New View 100 scanning white light interferometry microscope. Key specifications for this instrument are summarized in Table II

Table II  
WHITE LIGHT INSTRUMENT SPECIFICATION

Parameter	Description
Light source	Filtered White light
Camera size	640x480 pixels
Min vertical resolution	500 microns
Max vertical resolution	0.1 nm
Step height accuracy	1.5%
Repeatability	Better than 0.7 RMS
Objectives	2.5x and 40x Michelson objectives

### IV. SURFACE TOPOGRAPHY TO BRDF

In order to illustrate in detail the transformation from surface topography to BRDF, one sample is discussed in detail in what follows. Figure 2 shows the WLI topography measurements at two different magnifications (2.5x and 40x) obtained for a particular sample. Note that the images have been corrected for any systematic aberrations (piston, tilts, or spherical baselines) naturally arising in the WLI measurement. The RMS roughness is 2.48 nm for the 2.5x magnification and 1.23 for the 40x magnification

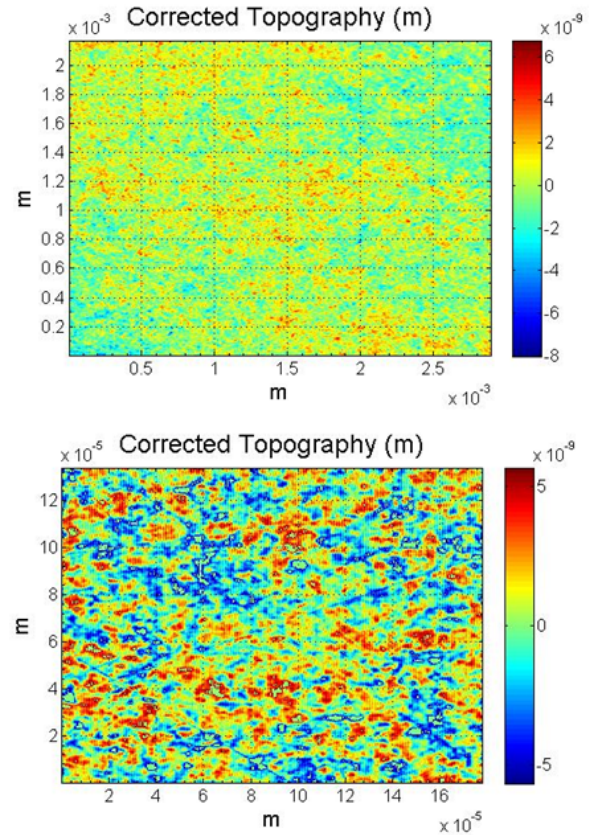


Figure 2. Topography for a particular sample at two different magnifications. Top: 2.5x magnification; RMS roughness = 1.23nm. Bottom: 40x magnification; RMS roughness = 2.48nm.

Using the topography information, the PSD for each magnification was computed using Eq. 3 and the results are graphically shown in Figure 3.

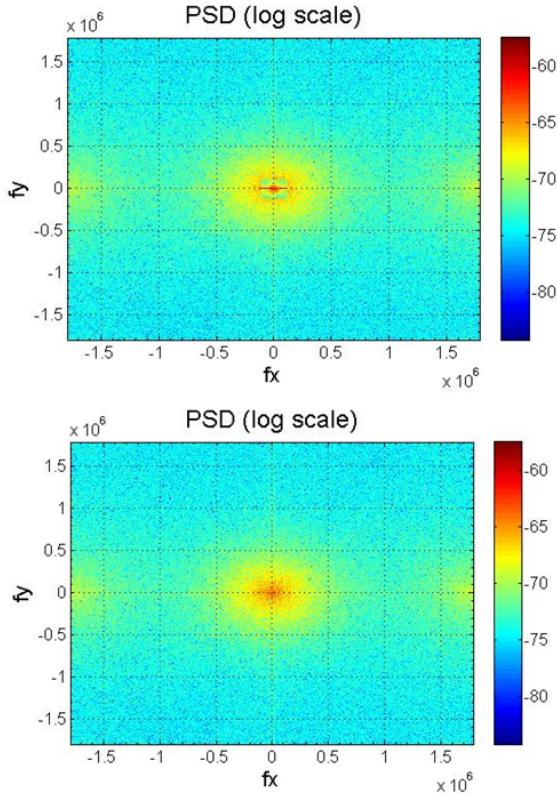


Figure 3. PSD for a particular sample. Top: PSD resulting from the 2.5x magnification. Bottom: PSD resulting from the 40x magnification

These topography profiles were then employed to compute the BRDF using Eq. 3. The following illumination and collection configuration were utilized during the calculation and correspond to those used for the experimental BRDF measurement:  $\lambda = 632nm$ ,  $\theta_{in} = 3^\circ$ , and  $\phi_s = 0$ . Additionally it was assumed that the reflectivity polarization factor was  $Q = 1$  since the experimentally determined BRDF did not discriminate between different polarizations.

Figure 4 shows the computed and the experimental BRDFs plotted on the same axis. The BRDF resulting from the 2.5x magnification covers only a region in the lower scattering angles whereas the BRDF for the higher magnification extends into larger scattering angles. This is as expected since the surface topography measured with the lower magnification covers the bandwidth of the low spatial frequencies of the surface, corresponding to low scattering angles, while with the higher magnification the high spatial frequencies will be measured, which consequently lead to high scatter angles.

## V. ACCURACY OF BRDF PREDICTION

In order to better understand the accuracy of the BRDF computation relative to the measured BRDF, for each inclination angle, the ratio of the computed BRDF to the experimentally determined BRDF was computed:

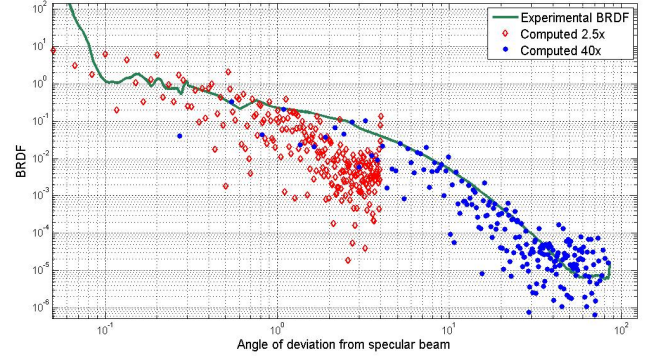


Figure 4. Comparison between computed and experimentally determined BRDF for one of the samples investigated

$$R(\theta_s) = \frac{BRDF_{comp}(\theta_s)}{BRDF_{experimental}(\theta_s)} \quad (6)$$

It is then convenient to characterize the accuracy of the BRDF computation by a single parameter defined by taking a logarithm based average over a useful range of scatter angles:

$$\bar{R} = \frac{1}{N} \sum_{\theta_s} \log[R(\theta_s)] \quad (7)$$

In general, inclination angles too close to the  $0.0^\circ$  fall within the laser signature, and inclination angles greater than  $80^\circ$  fall outside the collection angle of a typical optical system. Thus, as a general approximation, the useful range of angle lies between  $0.1^\circ < \theta_s < 80^\circ$ . For the case of a perfect agreement between computed and experimental BRDF,  $\bar{R} = 0.0$ . For the sample data discussed in the previous section, this value is  $\bar{R} = 1.1174$ .

All samples were analyzed in a similar fashion. The figure of merit,  $\bar{R}$  was obtained for each pair of experimental-computed BRDFs and the results are shown in Figure 7. Out of a total of 50 different cases, 43 feature  $\bar{R} < 1.0$ , implying that the overall accuracy of the BRDF computation is better than one order of magnitude.

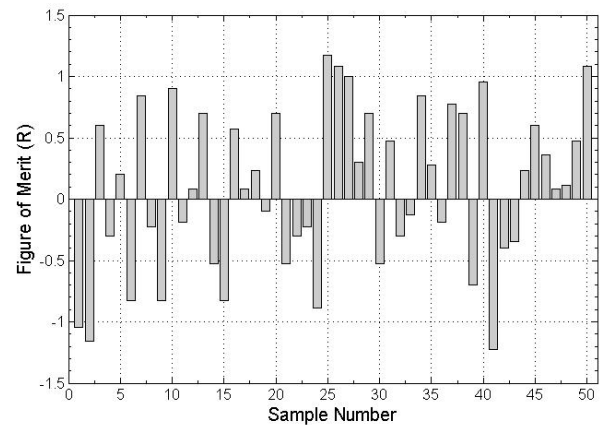


Figure 5. Figure of merit,  $\bar{R}$ , for the 50 different cases studied in this work.

In only 7 cases,  $\bar{R} > 1.0$  resulting in an overall computational accuracy slightly worse than 1 decade. For these 7 cases the disagreement between experiment and calculation are mostly due to odd features in the experimental BRDFs related to coatings, scattering from contaminants, sample defects, or anisotropic surface features. Another source of error is related to the fact that the BRDF and the WLI measurements were not spatially equivalent. This is not an issue for samples that are truly isotropic. However, for slightly anisotropic samples, it translates into small deviations between computed and measured BRDF. Across the entire population of samples investigated, the statistical mean is  $\bar{R}_{mean} = 0.0088$  with a the standard deviation of  $\sigma_{\bar{R}} = 0.65$

## VI. CONCLUSIONS

An efficient and accurate way of determining the BRDF of optical reflective samples (which are clean, front reflectors, and optically smooth) by employing a discretized form of the Rayleigh-Rice vector perturbation theory was demonstrated.

Fifty different pairs of experimental-computed BRDFs were examined and the accuracy of the BRDF computation was quantified by  $\bar{R}$  (defined in Eq. 7) . The sample's BRDF may be approximated using WLI measurements with a  $1\sigma$  confidence level of:

$$0.22 < BRDF < 4.46$$

## REFERENCES

- [1] J. C. Stover, *Optical Scattering: Measurement and Analysis*, 1995.
- [2] M. G. Dittman, "K-correlation power spectral density and surface scatter model," *Proc. of SPIE*, vol. 6291, 2006.